

Implementation of Two-Axis Position-Based Impedance Control with Inverse Kinematics Solution for A 2-DOF Robotic Finger

Khairunnisa Nasir, Ruhizan Liza Ahmad Shauri*, Norshariza Mohd Salleh, Nurul Hanani Remeli,

Faculty of Electrical Engineering, Universiti Teknologi MARA, 40450 Shah Alam, Selangor, Malaysia

*Corresponding author E-mail: ruhizan@salam.uitm.edu.my

Abstract

Position-based impedance control is a force control approach which consists of a single control law that accommodates the external force to achieve the desired dynamics of the body. A previously developed three-fingered robot hand was very rigid in its motion due to the application of position control alone. The position control scheme was inadequate for the tasks that involves the interaction of a robot end-effector with its environment which could damage fragile objects or be prone to slippage when provided with incorrect object's position. This paper introduces the application of two-axis position-based impedance control to one of the 2 degree-of-freedom (DOF) robotic finger of the robot hand. The goal of the control is to produce a mass-spring-dashpot system for the robot hand which considers the external force exerted by the object or environment onto the finger to modify the targeted position of the robot's tip-end. The position-based impedance control which was successfully performed however could not directly drive the DC-motors at the finger joints since it was expressed in the Cartesian position (X,Y,Z) form. Therefore, inverse kinematics was derived using geometrical approach to convert the Cartesian position (X,Y,Z) to angle position of motor which is controlled by PID. The proposed control and the developed kinematics were programmed using Matlab Simulink and tested in real-time experiments. The validation result has proven that the proposed position-based impedance control could modify the initial fingertip position according to the amount and direction of the applied external force, thus produced softness to the robotic finger.

Keywords: End-effector; force control; impedance control; inverse kinematics; robot finger; robot hand.

1. Introduction

Force control is very important for many robot manipulators as their practical manipulation tasks are normally associated with interaction between the end-effector of the robot and the environment. In current trend, robot manipulators are supposed to be more autonomous in which a simple motion control is inadequate to execute variety of manufacturing tasks where object sizes and positions may vary.

Various force control strategies have been developed for different research applications to satisfy the requirement of tasks performed by robots. According to Patel *et al.* [1], position control schemes are inadequate for the tasks that involves the interaction of a manipulator with its environment. Force control schemes are required to be developed in order to cater the task that demands extensive contact with the environment. Garcia *et al.* [2] claimed that in robotics manipulation task, manipulation can be performed only after the interaction forces are controlled properly, thus force control is required.

Impedance control is a well established force control scheme which was first introduced by Hogan [3] to establish a dynamical relationship between the force and robot end-effector position by regulating the mechanical impedance [4, 5]. According to Siciliano and Villani [6], to achieve a desired dynamic behavior, the impedance parameters known as mass, damping and stiffness need to be considered at the contact. An appropriate force/torque sensor usually mounted at the manipulator wrist is used to acquire information on the contact force and moment to keep linearity and

decoupling of the system during the interaction with the environment. Furthermore, the environmental forces and torques can be measured by a 6-DOF force-torque sensor mounted at the tip of the robot in usual industrial scenarios [7].

In principle, the end-effector can be controlled either as an actuator of force and torque or an actuator of position depending on the causality of the controller [8]. Controller with impedance causality is termed as force/torque-based impedance control while controller with causality of a mechanical admittance is termed as position-based impedance control [5, 8, 9]. In the force/torque-based impedance control, the end-effector is controlled by treating the mechanism as an actuator of force and torque to satisfy the impedance objective. The positional deviations are measured explicitly through position sensor while force and torque are commanded to actuate the end-effector [8, 10]. In contrast, the position-based impedance control controls the end-effector by treating the mechanism as an actuator of position. The position-based impedance control is a very well approach that suits for industrial robots as these robots are generally equipped with position controllers.

The previously developed robot hand was very rigid in its motion due to the application of position control alone [11]. Furthermore, the application of position control alone could damage fragile objects or be prone to slippage when provided with an incorrect object's position. This situation happens due to the absence of touch sensing ability of the robotic finger when interacting with the environment or an object. Therefore, this study introduces the position-based impedance control in two individual directions namely *x-axis* and *z-axis* focusing on one of the 2-DOF robotic finger only. The method aims to control the dynamic relation of the robot with the environment by regulating the force with ad-

adjustments made to the end-effector position to react the contact forces, which producing a mass-spring-dashpot system to the 2-DOF robotic finger. Prior to the position-based impedance control development, a new fingertip that embeds force sensors in x -axis and z -axis directions was designed in a separate study by Jaafar *et al.* [12] and Jaafar *et al.* [13]. Furthermore, calibration work for force measurement with the new design fingertip was successfully done in [14]. The position-based impedance control is implemented with PID position control for driving the motors through the inverse kinematics derivation. The inverse kinematics is derived to convert the modified position resulted from the position-based impedance control to angle references for actuation of DC-micromotors located at each joint of the robotic finger. The algorithms were developed in Matlab Simulink and validated through real-time experiments. Finally, the experimental results are analyzed and the discussions on the output system performance are presented.

2. Robot Hand Structure and System

The robot hand consists of a 1-DOF palm and three 2-DOF fingers which make the total of 7-DOF for the whole hand. One finger is fixed at the palm while the other two fingers are movable synchronously along the rotation of z -axis direction produced by the joint at the palm. Each finger has two joints actuated by

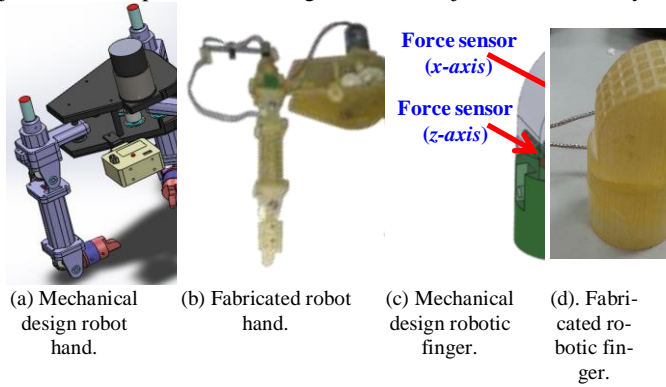


Fig. 1: Three-fingered robot hand [11] [13].

3. Position-Based Impedance Control

The position-based impedance control was developed by considering the translational impedance equation to enforce an equivalent mass-spring-dashpot behavior for the position displacement when the end-effector exerts a force on the environment as follows;

$$F_{ext} - F_{ref} = M_d(\Delta\ddot{P}) + D_d(\Delta\dot{P}) + K_d(\Delta P) \quad (1)$$

where the contact force for the robotic fingertip is given by the difference between the measured external force, F_{ext} and a fixed force

reference, F_{ref} . Meanwhile, M_d , D_d , K_d are the impedance parameters known as mass, damping and stiffness coefficients which were set at value of 1, 10 and 1000, respectively. $\Delta\ddot{P}$, $\Delta\dot{P}$, and ΔP represent the acceleration, velocity and position of the robotic fingertip, respectively.

A reference frame known as compliant frame Σ_c is introduced other than the desired frame Σ_d to describe the trajectory perturbation that takes the difference between the modified tip-end position P_c and desired tip-end positions P_d as demonstrated in equation (2). Equation (1) is used to compute ΔP and its associated derivatives with force information provided by the force sensors. The contact force for the robotic fingertip is taken from the differ-

ence between the measured external force, F_{ext} and a fixed force reference, F_{ref} . Rearranging equation (2) can be used to calculate P_c as shown in equation (3).

ence between the measured external force, F_{ext} and a fixed force reference, F_{ref} . Rearranging equation (2) can be used to calculate P_c as shown in equation (3).

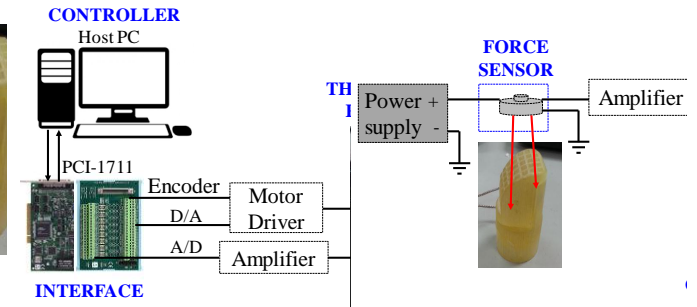


Fig. 2: System architecture of the three-fingered robot hand.

Fig. 3: System architecture of the three-fingered robot hand Force sensor circuitry.

ence between the measured external force, F_{ext} and a fixed force reference, F_{ref} . Rearranging equation (2) can be used to calculate P_c as shown in equation (3).

$$\Delta P = P_c - P_d \quad (2)$$

$$P_c = P_d + \Delta P \quad (3)$$

F_{ref} is used as a threshold to activate the position-based impedance control in which the desired position P_d will be modified to P_c when F_{ext} exceeded F_{ref} . When there is no interaction forces occurred on the robot's tip-end, there will be no trajectory perturbation, thus, $P_c = P_d$. Note that at this point, the position of the tip-end is resulted in the form of Cartesian position (X, Y, Z).

4. Inverse Kinematics

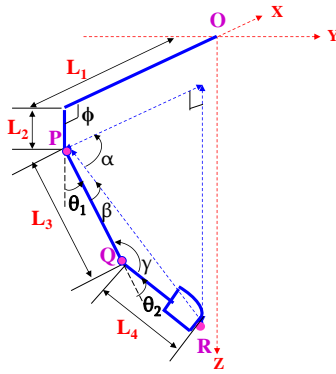
Inverse kinematics specifies the location of the robot's tip-end from the Cartesian position form by computing the associated joint angles of the robotic finger. It converts Cartesian position of tip-end (X, Y, Z) to joint angles for the fingers to actuate the motors at each joint of the robotic finger. Geometrical approach is used to solve the inverse kinematics for one of the 2-DOF robotic finger due to its capability of finding optimal solution with less computation. The diagram of the 2-DOF robotic finger is depicted in Fig. 4(a) which the condition of the tip-end position must be in

the ranges of X , Y , and Z are $-9.03 \text{ cm} < X < 7.1 \text{ cm}$; $Y = 0 \text{ cm}$ and $2.715 \text{ cm} < Z < 18.86 \text{ cm}$ to ensure that the robot's tip-end is within its reachability range. The point O is the origin of the robot hand while point R is the tip-end of the robotic finger. L_1 , L_2 , L_3 , and L_4 are the length dimensions from point O to R . Meanwhile, Fig. 4(b) presents the angles that contributed to the computation of θ_1 and θ_2 using geometrical approach by Saiki [15]. The calculations of θ_1 and θ_2 are shown in equations (4), and (5) which apply fixed angle ϕ and all the joint variables α , β , and γ as depicted in Fig. 4(a).

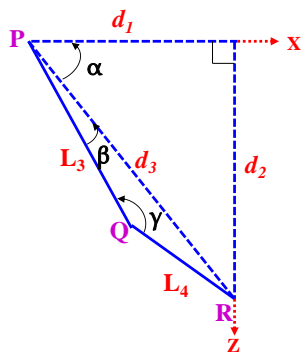
$$\theta_1 = 180^\circ - (\alpha + \beta + \phi) \quad (4)$$

$$\theta_2 = 180^\circ - \gamma \quad (5)$$

θ_1 is computed using equation (4) which involves the calculation of α , β and ϕ as in Fig. 4(b). ϕ is the fixed angle which was set at 90 deg ($^\circ$). Meanwhile, the joint variable α can be calculated using d_2 and d_3 through trigonometry and β can be obtained by cosine rule that involves calculation of L_1 , L_2 and d_3 . L_1 , and L_2 are known values however the value of d_3 depends on the d_1 and d_2 . The values of d_1 , d_2 and d_3 are regulated based on the position vector of R related to joint 1 with respect to z -axis and x -y axis. Therefore, d_3 can be determined using Pythagoras theorem. Finally, θ_2 is computed using equation (5) which involves γ depicted in Fig. 4(b). The cosine rule was also implemented to obtain γ .



(a) Diagram of the 2-DOF robot finger.



(b) Geometrical approach.

Fig. 4: Inverse kinematics solution.

5. Work Validation

The proposed method is validated by implementing the position-based impedance control together with position control to ensure that the commanded trajectory could perform successfully in the real-time experiment. The results are discussed in three phases including the validation of the proposed position based-impedance control, the inverse kinematics, and the combination of both with PID control. In this work, the parameters of the PID controller were set at $K_p = 0.8$, $K_i = 1.45$ and $K_d = 0.1$. All work phases are

integrated sequentially with one and another to create the complete robotic system as presented in Fig. 5.

P_d was provided in Cartesian form at $[X=0.04246; Y=0; Z=0.1245]$. Meanwhile, F_{ref} was specified at 1N for x -axis and 2N for z -axis to activate the developed impedance control in respective axis. When the impedance control output is activated, the P_d will be modified to P_c . Five random forces were applied and released to the robot's tip-end in the direction of x -axis and z -axis during the experiment using human finger. The output results from each integration phase were observed and analyzed to validate the proposed two-axis position-based impedance control in this study.

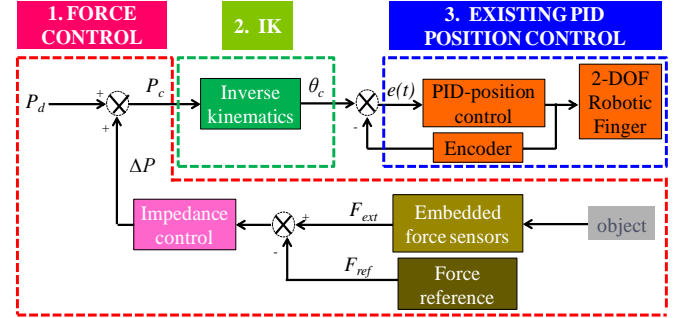
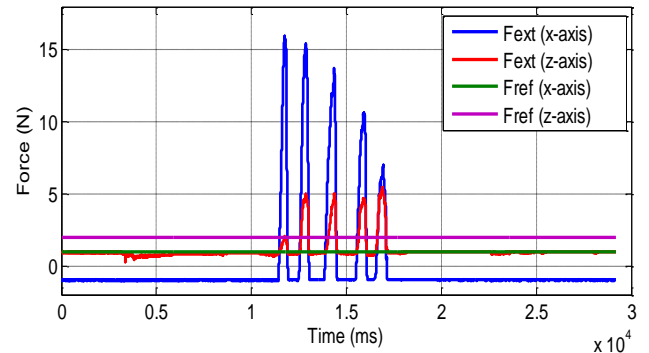


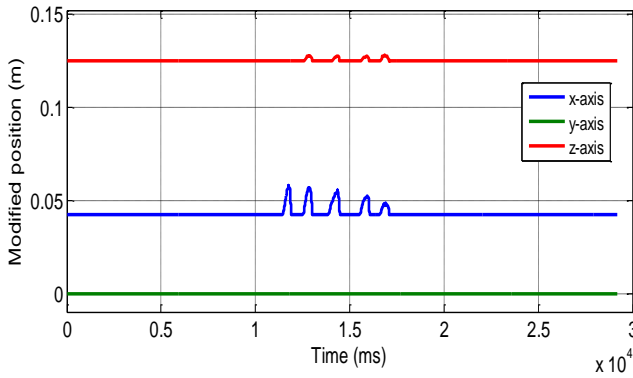
Fig. 5: Block Diagram of the 2-DOF Robotic Finger.

6. Results and Discussion

Fig. 6(a) shows the measured external force F_{ext} from the embedded force sensor while Fig. 6(b) is the result of modified tip-end position of the robotic finger from the proposed position-based impedance control. The blue line represents the output for x -axis direction while red line represents the output for z -axis direction. As can be seen in Fig. 6(a), the peaks occurred at time between 10s and 20s were resulted when random forces were applied and lifted from the robot's tip-end in both directions. Meanwhile, the result in Fig. 6(b) shows that when the external force in each axis was measured below their F_{ref} , the tip-end position was directed to the targeted position P_d which set to $[0.04246; 0; 0.1245]$. However, when the measured external force exceeded their F_{ref} , the P_d was modified to P_c according to the amount of force applied on the robot's tip-end. Referring to the x -axis position-based impedance control output result in Fig. 6(b), when the measured external force exceeded 1N , P_d was modified to P_c as presented by the five peaks. Meanwhile, the z -axis position-based impedance control output result shows that the first measured force applied did not exceed F_{ref} at 2N while other measured force applied exceeded 2N . From the graph, it can be clearly seen that instead of five, only four forces applied have affected P_d . The first force applied did not affect P_d because it did not exceed 2N . Conclusively, it can be observed that whenever the force applied exceeded its F_{ref} , P_d will be modified to P_c which depends on the amount of applied force to make the robotic finger behaves as a mass-spring-dashpot system.



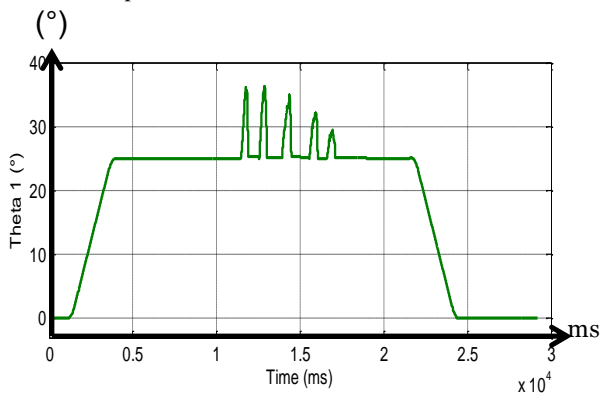
(a) Measured external force F_{ext} .



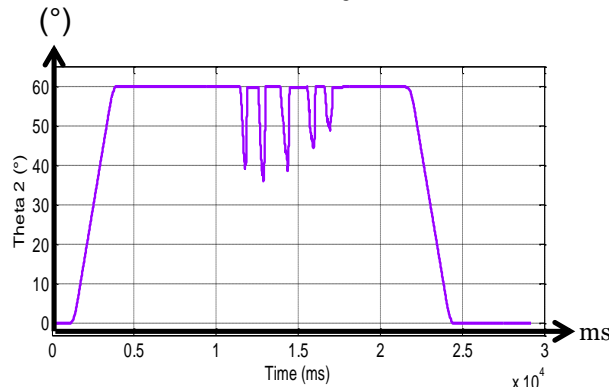
(b) Result of modified tip-end position.

Fig. 6: Result of developed position-based impedance control in x -axis and z -axis direction.

Next, P_c was provided to the derived inverse kinematics to convert the modified tip-end position into angle references to move the joints. The converted angles from P_c involved θ_1 and θ_2 as depicted in Fig. 7. According to the Fig. 7, the tip-end position was initially directed to 25° and 60° for θ_1 and θ_2 , respectively. θ_1 at 25° and θ_2 at 60° are the converted angles by the developed inverse kinematics from its targeted position P_d . Meanwhile, the peaks occurred between time 10s and 20s in both graphs were the converted angles of modified tip-end position P_c which resulted from the activation of position-based impedance control in both directions. During this time, θ_1 and θ_2 were affected as forces were applied according to Fig. 7 where θ_1 increased about 30° to 37° from its initial theta at 25° while θ_2 decreased about 49° to 36° from its initial theta at 60° . The changes on θ_1 and θ_2 show that the developed inverse kinematics worked successfully with the position-based impedance control.



(a) Converted angles of θ_1 .



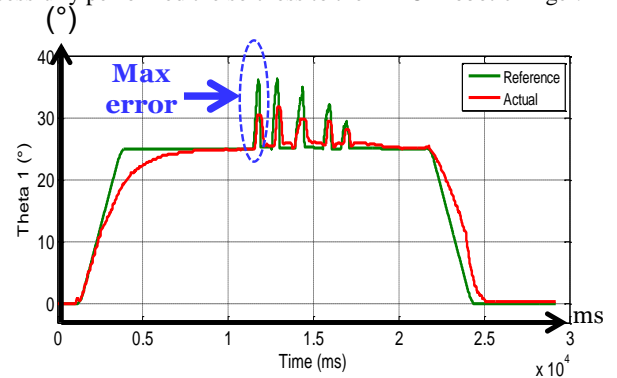
(b) Converted angles of θ_2 .

Fig. 7: Angles reference converted from tip-end position by the developed inverse kinematics.

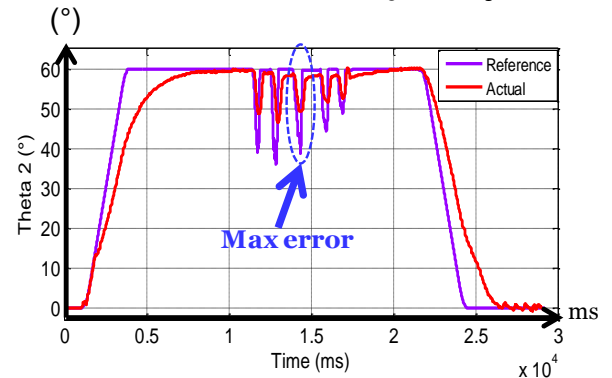
Finally, both converted angles were provided as the angle reference to the PID position control to actuate the finger joints by the DC-micromotors for impedance control validation purposes. The result is shown in Fig. 8. According to Fig. 8, the reference angles

are the commanded trajectory for motor actuation from the proposed two-axis position-based impedance control.

The commanded trajectory is labeled with green line for θ_1 and purple line for θ_2 . Meanwhile, the actual trajectory of motor actuation resulted from the PID position control is presented in red line for both thetas. From both graphs, it can be observed that the DC-micromotors tend to follow the commanded trajectory from the two-axis position-based impedance control. Small errors between the actual and commanded trajectory with the maximum of 5.5° and 10.5° respectively for θ_1 and θ_2 as shown in Fig. 8 were observed during 11s to 17s. This happened due to the inefficiency of the PID position control to catch up with the fast response of the force control. Even though the DC-micromotors did not exactly move according to the angle references, the actual trajectory is still able to follow the commanded trajectory. As can be seen in the duration between 10s and 20s, the 2-DOF robotic finger behaves as a mass-spring-dashpot system through the motion of the DC-micromotors when the tip-end position was modified according to the amount of applied force as shown in Fig. 6(a). Hence the proposed two-axis position-based impedance control is successfully performed the softness to the 2-DOF robotic finger.



(a) Result of driven motor using PID for θ_1 .



(b) Result of driven motor using PID for θ_2 .

Fig. 8: Real-time experiment result.

7. Conclusion

The proposed two-axis position-based impedance control has been developed on one of the 2-DOF finger of the three-fingered robot hand. The experimental result proved that the proposed two-axis position-based impedance control could provide softness to the 2-DOF robotic finger by modifying the targeted position P_d to a new tip-end position P_c when the measured external force F_{ext} exceeded the force reference F_{ref} . Furthermore, the derived inverse kinematics equation has correctly converted the finger's tip-end position in the form of Cartesian position (X,Y,Z) to the required position ($^\circ$) of motor at each joint. Then, once integrated with PID position control, the DC-micromotors was observed to follow the commanded trajectory with maximum position error of 5.5° and 10.5° , respectively for θ_1 and θ_2 . This was due to the inefficiency of the PID position control to catch up with the fast re-

sponse of force control will be investigated in the next study. Overall, the effectiveness of the proposed two-axis position-based impedance control and the inverse kinematics solution has been proven successful for the motion of actual robotic finger.

Acknowledgement

The authors gratefully acknowledge the support from Universiti Teknologi MARA in providing the Academic & Research Assimilation fund (600-RMI/DANA 5/3/ARAS (11/2015)). The authors would also thank the Faculty of Electrical Engineering, Universiti Teknologi MARA for providing equipments and other supports to conduct this research.

References

- [1] R. V. Patel, H. A. Talebi, J. Jayender, and F. Shadpey, "A Robust Position and Force Control Strategy for 7-DOF Redundant Manipulators," *IEEE/ASME Transactions on Mechatronics*, vol. 14, pp. 575-589, 2009.
- [2] J. G. Garcia, A. Robertsson, J. G. Ortega, and R. Johansson, "Force and Acceleration Sensor Fusion for Compliant Robot Motion Control," in *Proc. of the 2005 IEEE Int. Conf. on Robotics and Automation*, ICRA, 2005, pp. 2709-2714.
- [3] N. Hogan, "Impedance control of industrial robots," *Robotics and Computer-Integrated Manufacturing*, vol. 1, pp. 97-113, 1984.
- [4] H. Z. Arabshahi and A. B. Novinzadeh, "Impedance control of the 3RPS parallel manipulator," in *Second RSI/ISM Int. Conf. on Robotics and Mechatronics*, ICRoM, 2014, pp. 486-492.
- [5] C. Ott, R. Mukherjee, and Y. Nakamura, "Unified Impedance and Admittance Control," in *IEEE Int. Conf. on Robotics and Automation*, ICRA, 2010, pp. 554-561.
- [6] B. Siciliano and L. Villani, *Robot force control* vol. 540: Springer Science & Business Media, 2012.
- [7] C. Ott, *Cartesian impedance control of redundant and flexible-joint robots*: Springer, 2008.
- [8] D. A. Lawrence, "Impedance control stability properties in common implementations," in *Proc. IEEE Int. Conf. on Robotics and Automation*, 1988, pp. 1185-1190 vol.2.
- [9] J. Seul and T. C. Hsia, "Neural network impedance force control of robot manipulator," *IEEE Transactions on Industrial Electronics*, vol. 45, pp. 451-461, 1998.
- [10] M. G. Carmichael and D. Liu, "Admittance control scheme for implementing model-based assistance-as-needed on a robot," in *35th Ann. Int. Conf. of the IEEE Engineering in Medicine and Biology Society*, EMBC, 2013, pp. 870-873.
- [11] M. K. M. Kasim, R. L. A. Shauri, and K. Nasir, "PID position control of three-fingered hand for different grasping styles," in *IEEE 6th Control and System Graduate Research Colloquium*, ICSGRC, 2015, pp. 7-10.
- [12] J. J. a. R. L. A. Shauri, "Fingertip Structural Analysis-A Simulated Design Evaluation," *Jurnal Teknologi*, vol. 76, pp. 237-241, 2013.
- [13] J. Jaafar, K. Nasir, and R. L. A. Shauri, "Robot Hand Fingertip Design Validation," in *9th International Conference on Robotic, Vision, Signal Processing and Power Applications: Empowering Research and Innovation*, H. Ibrahim, S. Iqbal, S. S. Teoh, and M. T. Mustaffa, Eds., ed Singapore: Springer Singapore, 2017, pp. 647-653.
- [14] K. Nasir, R. L. A. Shauri, and J. Jaafar, "Calibration of embedded force sensor for robotic hand manipulation," in *2016 IEEE 12th Int. Colloquium on Signal Processing & Its Applications*, CSPA, 2016, pp. 351-355.
- [15] K. Saiki, "Autonomous assembly work by using arm robot with impedance control," Master's thesis, School of Engineering, Chiba University Graduate School of Engineering, 2012.